Eur. Phys. J. A (2016) **52**: 372
DOI 10.1140/epja/i2016-16372-x

THE EUROPEAN PHYSICAL JOURNAL A

Regular Article – Theoretical Physics

Structural and decay properties of $Z = 132, 138$ superheavy nuclei

Asloob A. Rather[1,a], M. Ikram[1], A.A. Usmani[1], Bharat Kumar[2,3], and S.K. Patra[2,3]

[1] Department of Physics, Aligarh Muslim University, Aligarh-202002, India
[2] Institute of Physics, Bhubaneswar-751 005, India
[3] Homi Bhabha National Institute, Anushakti Nagar, Mumbai-400094, India

Received: 21 October 2016 / Revised: 25 November 2016
Published online: 29 December 2016 –
Communicated by F. Gulminelli

Abstract. In this paper, we analyze the structural properties of $Z = 132$ and $Z = 138$ superheavy nuclei within the ambit of axially deformed relativistic mean-field framework with NL3* parametrization and calculate the total binding energies, radii, quadrupole deformation parameter, separation energies, density distributions. We also investigate the phenomenon of shape coexistence by performing the calculations for prolate, oblate and spherical configurations. For clear presentation of nucleon distributions, the two-dimensional contour representation of individual nucleon density and total matter density has been made. Further, a competition between possible decay modes such as α-decay, β-decay and spontaneous fission of the isotopic chain of superheavy nuclei with $Z = 132$ within the range $312 \leq A \leq 392$ and $318 \leq A \leq 398$ for $Z = 138$ is systematically analyzed within self-consistent relativistic mean-field model. From our analysis, we inferred that the α-decay and spontaneous fission are the principal modes of decay in majority of the isotopes of superheavy nuclei under investigation apart from β-decay as dominant mode of decay in $^{318-322}138$ isotopes.

1 Introduction

The quest for searching the limits on nuclear mass and charge in superheavy valley, which is still a largely unexplored area of research in nuclear physics, has been an intriguing endeavour for nuclear physics community from past several decades. Therefore, the discovery of new elements with atomic number $Z > 102$ in the laboratory is being pursued with great vigour nowadays. The existence of superheavy nuclei (SHN) is the result of the interplay of the attractive nuclear force and the disruptive Coulomb repulsion between protons that favours fission. In principle, for SHN the shape of the classical nuclear droplet which is governed by surface tension and Coulomb repulsion is unable to withstand the surface distortions making these nuclei susceptible to spontaneous fission. Thus, the stability of superheavy elements has become a long-standing fundamental nuclear science problem. Some of the topical issues that the nuclear physics community is looking to address in the superheavy regime of the nuclear chart are: how a nucleus with a large atomic number, such as $Z = 112$, survives the huge electrostatic repulsion between the protons, its physical and chemical properties, the extent of the superheavy region, *i.e.*, to find an upper limit on the number of neutrons and protons that can be bound into one cluster, and the existence of very long-lived superheavy nuclei. Theoretically, the mere existence of the heaviest elements with $Z > 102$ is entirely due to quantal shell effects. However, in the mid-sixties, with the invention of the shell-correction method, it was established that long-lived superheavy elements (SHE) with very large atomic numbers could exist due to the strong shell stabilization [1–5]. By incorporating shell effects, it shall be quite interesting to explore the regions in (Z, N)-plane where long-lived superheavy nuclei might be expected. Exploration of the (Z, N)-plane in the superheavy valley is driven by the understanding of not only the nuclear structure but also the structure of stars and the evolution of universe. Pursuing this line of thought, the pioneering work on superheavy elements was performed in 1960s [1, 3–5] and such studies were quite successful in reproducing the already known half-lives by employing macroscopic-microscopic method (Nilsson-Strutinsky approach) with the folded-Yukawa deformed single-particle potential [6,7] and with the Woods-Saxon deformed single-particle potential [8–10]. Further, the outcome of these exhaustive investigations led to the understanding that the valley of superheavy nuclei is separated in proton and neutron number from known heavy

[a] e-mail: asloobahmad.rs@amu.ac.in

elements by a region of much higher instability. In addition, several theoretical models which come under the aegis of macro-micro method like the fission model [11], cluster model [12], the density-dependent M3Y(DDM3Y) effective model [13], the generalized liquid drop model (GLDM) [14], etc. and self-consistent models like the relativistic mean-field (RMF) theory [15], Skyrme Hartree-Fock (SHF) model [16], etc. proved to be an effective tool for the successful description of α-decay from heavy and SHN.

From past three decades, the experimentalists have launched an expedition for predicting the "island of superheavy elements", a region of increasing stable nuclei around $Z = 114$, which has led to a burst of intense activity in the superheavy regime. The synthesis of SHN in laboratory is accomplished by fusion of heavy nuclei above the barrier [17]. The two main processes employed for the synthesis of SHN are cold fusion performed mainly at GSI, Darmstadt and RIKEN Japan and hot-fusion reactions performed at JINR-FLNR, Dubna. Until now, SHN with $Z \leq 118$ have been synthesized in the laboratory. The elements with $Z = 110$, 111 and 112 were produced in the experiments carried out at GSI [18–22]. The fusion cross section was extremely small in production of $Z = 112$ nucleus which led to the conclusion that the formation of further heavier elements would be very difficult by this process. The element with $Z = 113$ was identified at RIKEN, Japan [23, 24] using the cold-fusion reaction with a very low cross section ~ 0.03 pb thus confirming the limitation of cold-fusion technique. The synthesis of $Z = 113$–118 was performed successfully by the experimentalists from joint collaboration of JINR-FLNR, Dubna and Lawrence Liverpool National Laboratory along with an unsuccessful attempt on the production of $Z = 120$ through the hot-fusion technique [25–28]. The isotopes of elements $Z = 112$, 114, 116 and 118 were identified in fusion-evaporation reactions at low excitation energies by irradiation of ^{233,238}U, ^{242}Pu, ^{248}Cm and ^{248}Cf with ^{48}Ca beams [29]. The element $Z = 118$ and its immediate decay product, element with $Z = 116$, were produced at Berkeley Lab's 88 inch cyclotron by bombarding targets of lead with an intense beam of high-energy krypton ions. The element ^{270}Hs with $Z = 108$ and $N = 162$ was synthesized by Dvorak *et al.* [30] by $^{26}\mathrm{Mg} + {}^{248}\mathrm{Cm}$ reaction. Although the advancement in the accelerator facilities and the nuclear beam technologies have pushed the frontiers of nuclear chart especially in the superheavy region upto a great extent except for an attempt [31] to produce $Z = 120$ superheavy nuclei through the reaction $^{244}\mathrm{Pu} + {}^{58}\mathrm{Fe}$, there has been until now no evidence for the production of nuclei with $Z > 118$. The short lifetimes and the low production cross sections observed in fusion evaporation residues often increases the difficulty in synthesis of new superheavy nuclei and are posing a major difficulty to both theoreticians and experimentalists in understanding the various properties of superheavy nuclei.

Superheavy nuclei and their decay properties is one of the fastest growing fields in nuclear science nowadays. The discovery of alpha decay by Becquerel in 1896 and subsequently the alpha theory of decay proposed by Gamow, Condon and Gurnay in 1928 has ushered a new era in nuclear science. Quantum mechanically, α-decay occurs in heavy and superheavy nuclei by tunnelling process through a Coulomb barrier which is classically forbidden. The alpha decay [14, 32–36] of the SHN is possible only if the shell effect supplies the extra binding energy and increases the barrier height of the fission. Thus, the beta stable nuclei with relatively longer half-life for spontaneous fission than that of alpha decay indicate that the dominant decay mode for such a superheavy nucleus might be alpha decay. It is worth mentioning here that the α-decay is not the only mode of decay found in heavy nuclei but there is wealth of literature for β-decay, spontaneous fission (SF) and cluster decay also for such nuclei [37–45]. Generally, alpha decay occurs in heavy and superheavy nuclei whereas beta decay can occur throughout the periodic chart. The understanding of spontaneous fission and alpha decay on superheavy nuclei is rather more important than beta decay because the SHN with relative small alpha decay half-lives compared to SF half-lives will survive the fission and thus can be observed in the laboratory through alpha decay. Hence, the α-decay plays an indispensable role in the identification of new superheavy elements. Besides this, it has also been predicted that beta decay may play an important role for some of the superheavy nuclei [46]. However, β-decay proceeds through a weak interaction, the process is slow and less favoured compared to SF and alpha decay.

It is worth mentioning that the alpha decay and spontaneous fission are the main decay modes for both heavy and superheavy nuclei with $Z > 92$. The spontaneous fission acts as the limiting factor that decides the stability of superheavy nuclei and hence puts a limit on the number of chemical elements that can exist. It was Bohr and Wheeler [47] in 1939 who predicted and described the mechanism of spontaneous fission process on the basis of liquid drop model and established a limit of $\frac{Z^2}{A} \approx 48$, beyond which nuclei are unstable against spontaneous fission, and later in 1940, Flerov *et al.* [48] observed this phenomenon in ^{235}U. This was followed by the several empirical formulas being proposed by various authors for calculating the half-lives in spontaneous fission and the first attempt in this direction was made by Swiatecki [49] who proposed a semi-empirical formula for spontaneous fission. Further, Ren *et al.* [50, 51] proposed a phenomenological formula for calculating the spontaneous fission half-lives, and recently Xu *et al.* [52] generalized an empirical formula for spontaneous fission half-lives of even-even nuclei. Here, in present manuscript, within the structural studies we made an attempt to look for the competition among various possible modes of decay such as α-decay, β-decay and SF of the isotopes of $Z = 132$ and $Z = 138$ superheavy elements with a neutron range $180 \leq N \leq 260$ and predict the possible modes of decay. The contents of the manuscript are organized as follows. The framework of relativistic mean-field formalism is outlined in sect. 2. The results and discussion is presented in sect. 3. Finally, sect. 4 contains the main summary and conclusions of this work.

2 Theoretical formalism

From last few decades, the RMF theory has achieved a great success in describing many of the nuclear phenomena. Over the nonrelativistic case, it is quite better to reproduce the structural properties of nuclei throughout the periodic table [53–57] near or far from the stability lines including superheavy region [58]. The starting point of the RMF theory is the basic Lagrangian containing nucleons interacting with σ-, ω- and ρ-meson fields. The photon field A_μ is included to take care of the Coulomb interaction of protons. The relativistic mean-field Lagrangian density is expressed as [53–57],

$$\begin{aligned}\mathcal{L} = {} & \bar{\psi}_i\{i\gamma^\mu\partial_\mu - M\}\psi_i + \frac{1}{2}\partial^\mu\sigma\partial_\mu\sigma - \frac{1}{2}m_\sigma^2\sigma^2 - \frac{1}{3}g_2\sigma^3 \\ & -\frac{1}{4}g_3\sigma^4 - g_s\bar{\psi}_i\psi_i\sigma - \frac{1}{4}\Omega^{\mu\nu}\Omega_{\mu\nu} + \frac{1}{2}m_w^2V^\mu V_\mu \\ & -g_w\bar{\psi}_i\gamma^\mu\psi_iV_\mu - \frac{1}{4}\boldsymbol{B}^{\mu\nu}\boldsymbol{B}_{\mu\nu} + \frac{1}{2}m_\rho^2\boldsymbol{R}^\mu\boldsymbol{R}_\mu - \frac{1}{4}F^{\mu\nu}F_{\mu\nu} \\ & -g_\rho\bar{\psi}_i\gamma^\mu\boldsymbol{\tau}\psi_i\boldsymbol{R^\mu} - e\bar{\psi}_i\gamma^\mu\frac{(1-\tau_{3i})}{2}\psi_iA_\mu. \end{aligned} \quad (1)$$

Here M, m_σ, m_ω and m_ρ are the masses for nucleon, σ-, ω- and ρ-mesons and ψ is the Dirac spinor. The field for the σ-meson is denoted by σ, ω-meson by V_μ and ρ-meson by R_μ. g_s, g_ω, g_ρ and $e^2/4\pi = 1/137$ are the coupling constants for the σ, ω, ρ-mesons and photon, respectively. g_2 and g_3 are the self-interaction coupling constants for σ-mesons. By using the classical variational principle, we obtain the field equations for the nucleons and mesons:

$$\begin{aligned} \{-\Delta + m_\sigma^2\}\sigma^0(r_\perp, z) = {} & -g_\sigma\rho_s(r_\perp, z) \\ & -g_2\sigma^2(r_\perp, z) - g_3\sigma^3(r_\perp, z), \quad (2) \\ \{-\Delta + m_\omega^2\}V^0(r_\perp, z) = {} & g_\omega\rho_v(r_\perp, z), \quad (3) \\ \{-\Delta + m_\rho^2\}R^0(r_\perp, z) = {} & g_\rho\rho_3(r_\perp, z), \quad (4) \\ -\Delta A^0(r_\perp, z) = {} & e\rho_c(r_\perp, z). \quad (5) \end{aligned}$$

The Dirac equation for the nucleons is written by

$$\{-i\alpha\nabla + V(r_\perp, z) + \beta M^\dagger\}\psi_i = \epsilon_i\psi_i. \quad (6)$$

The effective mass of the nucleon is

$$M^\dagger = M + S(r_\perp, z) = M + g_\sigma\sigma(r_\perp, z), \quad (7)$$

and the vector potential is

$$\begin{aligned} V(r_\perp, z) = {} & g_\omega V^0(r_\perp, z) + g_\rho\tau_3R^0(r_\perp, z) \\ & + e\frac{(1-\tau_3)}{2}A^0(r_\perp, z). \end{aligned} \quad (8)$$

A static solution is obtained from the equations of motion to describe the ground state properties of nuclei. The set of nonlinear coupled equations are solved self-consistently in an axially deformed harmonic oscillator basis $N_F = N_B = 20$. The quadrupole deformation parameter β_2 is extracted from the calculated quadrupole moments of neutrons and protons through

$$Q = Q_n + Q_p = \sqrt{\frac{16\pi}{5}}\left(\frac{3}{4\pi}AR^2\beta_2\right), \quad (9)$$

where $R = 1.2A^{1/3}$.

The total energy of the system is given by

$$E_{total} = E_{part} + E_\sigma + E_\omega + E_\rho + E_c + E_{pair} + E_{c.m.}, \quad (10)$$

where E_{part} is the sum of the single-particle energies of the nucleons and E_σ, E_ω, E_ρ, E_c, E_{pair}, E_{cm} are the contributions of the meson fields, the Coulomb field, pairing energy and the center-of-mass energy, respectively. In present calculations, we use the constant gap BCS approximation to take care of pairing interaction [59]. We use nonlinear NL3* parameter set [60] throughout the calculations.

3 Results and discussions

In this paper, we performed self-consistent relativistic mean-field calculations by employing NL3* for calculating the binding energy, radii and quadrupole deformation β_2 for three different shape configurations. In refs. [61, 62], $Z = 132$, 138 are suggested to be proton and $N = 198$, 228, 238 and 258 are neutron magic numbers. Therefore, we considered a neutron range $N = 180$–260 that covers all these neutron magic numbers. These neutron as well as proton magic numbers form the doubly magic systems as $^{330}132$, $^{360}132$, $^{370}132$, $^{366}138$, $^{376}138$ and $^{396}138$. To analyze the structural properties of these isotopes, we made an attempt using deformed RMF calculations. It is well known that the superheavy nuclei are identified by α-decay in the laboratory followed by spontaneous fission. Therefore, to predict the possible mode of decay for the considered range of nuclides we make an investigation to analyze the competition between α-decay, β-decay and spontaneous fission which is considered to be the central theme of the paper. The results are explained in sects. 3.1–3.6.

3.1 Selection of basis space

The RMF Lagrangian is used to obtain Dirac equation for fermions and the Klein-Gordon equations for bosons using state-of the art variational approach in a self-consistent manner. Further, these equations are solved in an axially deformed harmonic oscillator basis N_F and N_B for fermionic and bosonic wave function, respectively. For superheavy nuclei, a large number of basis space N_F and N_B is needed to get a convergent solution. For this, we have to choose an optimal model space for both fermion and boson fields. To choose optimal values for N_F and N_B, we select $^{312,380}132$ systems as a test case and increase the basis number from 8 to 20 step by step. Results obtained for $^{312,380}132$ systems using these bases are

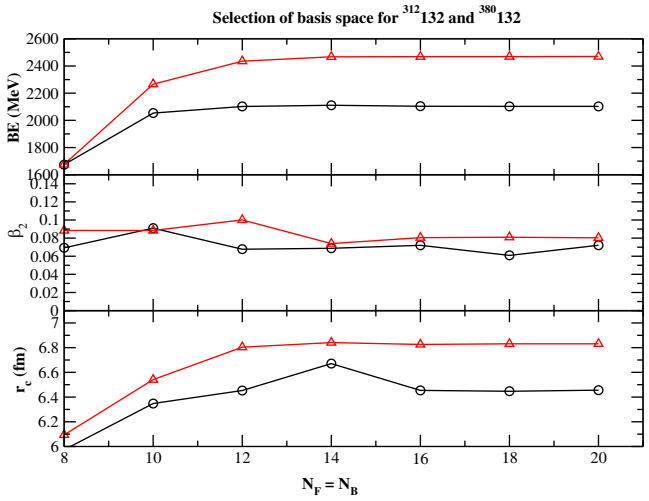

Fig. 1. (Color online) The variation of calculated binding energy (BE), and quadrupole deformation parameter (β_2) and charge radius (r_c) are given with bosonic and fermionic basis. Black lines with circles represent the results for ^{312}132 and the results of ^{380}132 are shown by red lines with triangles.

shown in fig. 1. From our calculations, we notice an increment of 379 MeV in binding energy while going from $N_F = N_B = 8$ to 10 for ^{312}132 system and it comes to be 48 MeV while N_F and N_B change from 10 to 12 and further by increasing the number of basis a constant value of BE is obtained. Proceeding along the similar lines, for ^{380}132 system, we notice a large increment in binding energy around 590 MeV when the bases change from 8 to 10 and this amount of BE reduces to 170 MeV while the bases (N_F and N_B) change from 10 to 12 and further a constant value of BE is obtained by increasing the basis space. This increment in energy decreases while going to higher oscillator basis. For example, change in binding energy is $\approx$ 0.2 and 0.6 MeV for ^{312}132 and ^{380}132, respectively, with a change of $N_F = N_B$ from 18 to 20. Therefore, the present calculations dictate that the optimal basis to be chosen is $N_F = N_B = 20$ which is well within the convergence limits of the current RMF models.

3.2 Binding energy, radii and quadrupole deformation parameter

The calculated binding energy, radii and the quadrupole deformation parameter for the isotopic chains $^{312-392}$132 and $^{318-398}$138 are given in tables 1, 2 and plotted in figs. 2, 3. To find the ground state solution, the calculations are performed with an initial spherical, prolate and oblate quadrupole deformation parameter β_0 in the relativistic mean-field formalism. It is important to mention here that maximum binding energy corresponds to the ground state energy and all other solutions are the intrinsic excited state configurations. Proceeding along these lines, we found prolate as a ground state for most of the cases. As the experimental binding energies for these superheavy isotopic chains are not available, in order to provide some validity to the predictive power of

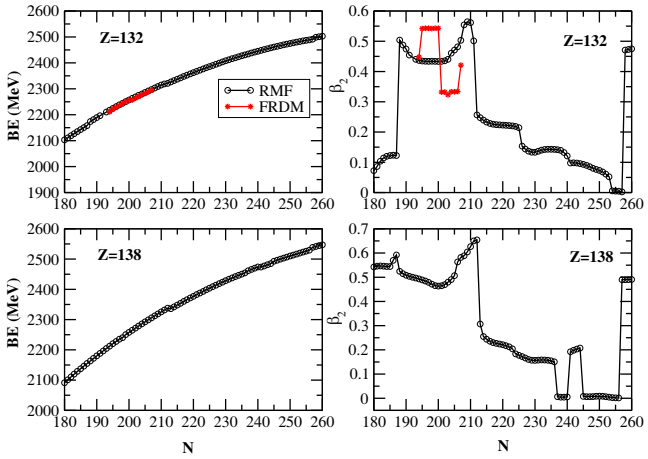

Fig. 2. (Color online) Binding energy and deformation parameter as a function of neutron number.

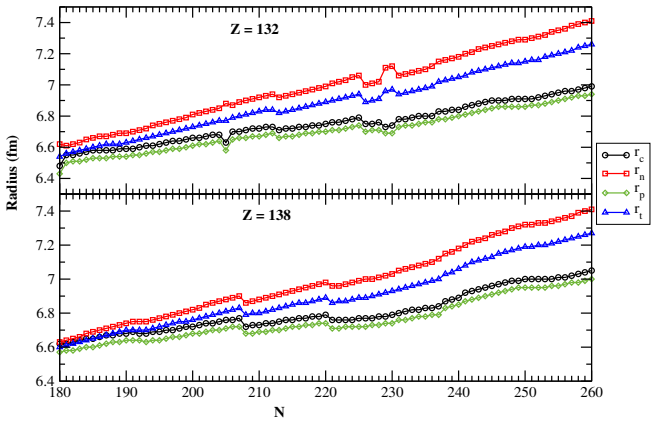

Fig. 3. (Color online) Radii as a function of neutron number.

our calculations a comparison of binding energies of our calculations with those obtained from finite range droplet model (FRDM) [6,7] is made wherever available and close agreement is found. The calculated quadrupole deformation parameter from RMF and the values obtained from FRDM [6,7] predict the ground state of the considered isotopic chains to be prolate, however, there is a difference in magnitude, as indicated in table 1 as well as in fig. 2. The radii monotonically increases with increasing number of neutrons. In general, the calculated binding energies are in good agreement with those of the FRDM values wherever available.

3.3 Separation energy

The separation energy is an important observable in identifying the signature of magic numbers in nuclei. The magic numbers in nuclei are characterized by large shell gaps in their single-particle energy levels. This implies that the nucleons occupying the lower energy level have comparatively large value of energy than those nucleons occupying the higher energy levels, giving rise to more stability. The extra stability attributed to certain numbers can be

Table 1. Binding energy, deformation parameter and radii for $Z = 132$ isotopic chain within three possible shape configurations.

Nuclei	BE			β_2			r_c			r_t			FRDM	
	sph.	prol.	obl.	sph.	prol.	obl.	sph.	prol	obl.	sph.	prol.	obl.	BE	β_2
^{312}132	2103.0		2159.2	0.073		−0.208	6.457		6.480	6.479		6.543		
^{313}132	2111.0		2118.0	0.086		−0.251	6.469		6.546	6.493		6.561		
^{314}132	2119.0		2126.0	0.102		−0.254	6.483		6.554	6.508		6.572		
^{315}132	2127.0		2133.8	0.112		−0.257	6.494		6.562	6.521		6.583		
^{316}132	2134.9		2141.4	0.118		−0.259	6.503		6.569	6.532		6.593		
^{317}132	2142.7		2148.9	0.121		−0.259	6.511		6.575	6.543		6.602		
^{318}132	2150.4		2156.2	0.122		−0.258	6.519		6.580	6.553		6.610		
^{319}132	2157.9		2163.5	0.121		−0.253	6.525		6.583	6.562		6.616		
^{320}132	2165.2	2173.8	2170.8	0.118	0.496	−0.245	6.531	6.753	6.584	6.571	6.783	6.620		
^{321}132	2172.4	2181.3	2178.1	0.113	0.480	−0.237	6.535	6.744	6.585	6.578	6.778	6.624		
^{322}132	2179.6	2188.7	2185.4	0.104	0.467	−0.233	6.536	6.739	6.589	6.584	6.776	6.631		
^{323}132	2186.6	2196.0	2192.6	0.091	0.447	−0.232	6.535	6.729	6.594	6.587	6.769	6.639		
^{324}132	2193.7	2196.0	2199.7	0.080	0.447	−0.232	6.535	6.729	6.600	6.591	6.769	6.648		
^{325}132	2200.7	2210.4	2206.7	0.072	0.433	−0.232	6.538	6.729	6.607	6.598	6.775	6.657		
^{326}132	2207.7	2217.4	2213.6	0.067	0.429	−0.233	6.544	6.732	6.613	6.606	6.781	6.667	2211.5	0.448
^{327}132	2214.6	2224.4	2220.3	0.061	0.425	−0.234	6.550	6.736	6.620	6.615	6.788	6.677	2221.5	0.542
^{328}132	2221.3	2231.1	2226.9	0.057	0.420	−0.236	6.556	6.741	6.628	6.624	6.797	6.687	2229.3	0.543
^{329}132	2227.8	2237.8	2233.4	0.050	0.421	−0.238	6.563	6.747	6.635	6.633	6.806	6.697	2235.8	0.543
^{330}132	2234.3	2244.3	2239.7	0.000	0.428	−0.239	6.569	6.754	6.642	6.641	6.816	6.707	2243.4	0.542
^{331}132	2240.7	2250.7	2245.9	0.000	0.428	−0.241	6.577	6.761	6.649	6.651	6.826	6.718	2249.6	0.543
^{332}132	2246.7	2256.8	2252.1	0.000	0.426	−0.242	6.584	6.768	6.657	6.661	6.835	6.728	2256.9	0.543
^{333}132	2252.5	2262.9	2258.2	0.007	0.427	−0.244	6.591	6.776	6.664	6.671	6.846	6.738	2256.9	0.332
^{334}132	2258.4	2268.7	2264.2	0.031	0.429	−0.245	6.598	6.785	6.671	6.680	6.858	6.748	2264.1	0.332
^{335}132	2264.4	2274.5	2270.1	0.051	0.434	−0.246	6.605	6.795	6.677	6.690	6.871	6.758	2269.9	0.323
^{336}132		2280.1	2275.9		0.455	−0.248		6.817	6.684		6.896	6.767	2276.6	0.333
^{337}132		2285.9	2294.1		0.469	−0.186		6.832	6.627		6.914	6.771	2281.9	0.333
^{338}132		2291.6	2287.2		0.480	−0.251		6.780	6.697		6.933	6.787	2288.6	0.334
^{339}132		2297.2	2292.7		0.494	−0.253		6.875	6.703		6.962	6.797	2294.3	0.421
^{340}132		2303.2	2298.1		0.514	−0.255		6.933	6.710		7.021	6.807		
^{341}132		2308.8	2303.5		0.525	−0.257		6.949	6.716		7.040	6.817		
^{342}132		2314.1	2308.7		0.516	−0.259		6.950	6.722		7.045	6.827		
^{343}132		2318.9	2314.0		0.456	−0.261		6.898	6.728		6.997	6.836		
^{344}132		2321.0	2319.1		0.258	−0.260		6.707	6.733		6.819	6.844		
^{345}132		2326.3	2324.0		0.248	−0.202		6.707	6.712		6.823	6.823		
^{346}132		2331.6	2329.2		0.240	−0.201		6.709	6.717		6.828	6.831		
^{347}132		2336.9	2334.4		0.233	−0.202		6.713	6.722		6.834	6.840		
^{348}132		2342.2	2339.4		0.229	−0.203		6.717	6.727		6.841	6.849		
^{349}132		2347.3	2344.3		0.226	−0.205		6.721	6.732		6.849	6.858		
^{350}132		2352.4	2349.2		0.225	−0.207		6.726	6.738		6.857	6.867		
^{351}132		2357.4	2354.0		0.224	−0.209		6.731	6.743		6.866	6.876		
^{352}132		2362.3	2358.7		0.223	−0.212		6.735	6.749		6.874	6.886		
^{353}132		2367.2	2363.4		0.222	−0.216		6.740	6.755		6.883	6.896		
^{354}132		2371.8	2368.1		0.222	−0.221		6.745	6.761		6.892	6.906		
^{355}132	2373.5	2376.5	2372.8	−0.01	0.219	−0.227	6.732	6.750	6.769	6.868	6.900	6.918		
^{356}132		2381.0	2377.4		0.217	−0.237		6.755	6.780		6.909	6.932		
^{357}132		2385.4	2382.0		0.214	−0.242		6.759	6.789		6.916	6.944		
^{358}132		2389.9			0.155			6.748			6.906			
^{359}132	2393.8	2394.5		0.001	0.145		6.752	6.752		6.901	6.913			
^{360}132	2398.6	2399.1		0.001	0.138		6.758	6.757		6.910	6.921			
^{361}132	2403.0	2403.6	2387.6	0.001	0.135	−0.134	6.764	6.763	6.734	6.920	6.929	6.964		
^{362}132	2407.1	2407.9	2391.0	0.002	0.135	−0.139	6.770	6.768	6.739	6.929	6.938	6.974		
^{363}132	2411.3	2412.0		0.005	0.136		6.777	6.773		6.939	6.948			
^{364}132	2415.4	2416.0		0.014	0.140		6.783	6.777		6.949	6.957			
^{365}132	2419.5	2419.9		0.023	0.142		6.790	6.782		6.959	6.966			
^{366}132	2423.6	2423.7		0.024	0.143		6.796	6.786		6.969	6.976			
^{367}132	2427.6	2427.4		0.013	0.143		6.803	6.791		6.979	6.985			

Table 1. Continued.

Nuclei	BE			β_2			r_c			r_t		
	sph.	prol.	obl.	sph.	prol.	obl.	sph.	prol	obl.	sph.	prol.	obl.
^{368}132	2431.6	2431.1	2430.2	0.004	0.143	−0.083	6.81	6.796	6.803	6.989	6.994	6.988
^{369}132	2435.5	2434.6	2433.4	0.002	0.142	−0.172	6.816	6.8	6.825	6.999	7.003	7.015
^{370}132	2439.3	2438.2	2437.5	0.001	0.139	−0.176	6.822	6.804	6.831	7.008	7.011	7.026
^{371}132	2442.6	2441.5	2441.5	0.001	0.132	−0.179	6.825	6.806	6.837	7.017	7.017	7.036
^{372}132	2445.6	2444.8	2445.3	0.002	0.121	−0.183	6.828	6.806	6.843	7.025	7.022	7.046
^{373}132	2448.5		2448.8	0.003		−0.197	6.83		6.855	7.033		7.061
^{374}132	2451.4		2452.4	0.005		−0.214	6.831		6.870	7.041		7.077
^{375}132	2454.3		2455.9	0.009		−0.223	6.833		6.881	7.049		7.091
^{376}132	2457.2		2459.2	0.019		−0.229	6.834		6.891	7.056		7.104
^{377}132	2460.8		2462.2	0.092		−0.230	6.821		6.897	7.058		7.114
^{378}132	2463.8		2464.6	0.089		−0.228	6.824		6.902	7.066		7.122
^{379}132	2466.7		2467.6	0.084		−0.224	6.827		6.904	7.074		7.129
^{380}132	2469.6		2470.3	0.079		−0.218	6.831		6.906	7.083		7.135
^{381}132	2472.3		2473.1	0.076		−0.213	6.834		6.908	7.091		7.141
^{382}132	2475.1		2475.8	0.072		−0.209	6.837		6.910	7.099		7.148
^{383}132	2477.6		2478.6	0.067		−0.205	6.839		6.913	7.107		7.155
^{384}132	2479.9		2481.3	0.060		−0.205	6.841		6.918	7.115		7.164
^{385}132	2482.3		2483.9	0.051		−0.208	6.842		6.926	7.123		7.175
^{386}132	2484.7		2486.5	0.002		−0.213	6.853		6.936	7.137		7.187
^{387}132	2486.9		2488.9	0.002		−0.219	6.853		6.946	7.144		7.199
^{388}132	2488.9		2491.5	0.002		−0.224	6.852		6.955	7.151		7.212
^{389}132	2491.2		2494.0	0.001		−0.228	6.851		6.964	7.158		7.223
^{390}132	2493.2	2498.8	2496.4	0.001	0.471	−0.231	6.851	7.132	6.972	7.165	7.383	7.235
^{391}132	2495.2	2500.9	2498.5	0.000	0.473	−0.234	6.857	7.141	6.980	7.175	7.395	7.246
^{392}132	2496.8	2502.9	2500.4	0.007	0.475	−0.237	6.867	7.149	6.989	7.186	7.407	7.257
^{393}132	2498.7	2504.8	2502.4	0.029	0.477	−0.240	6.879	7.158	6.998	7.197	7.419	7.269
^{394}132	2500.8	2506.7	2504.3	0.046	0.479	−0.243	6.893	7.167	7.007	7.210	7.432	7.281
^{395}132	2502.9	2508.7	2506.1	0.056	0.482	−0.247	6.907	7.176	7.016	7.222	7.444	7.293

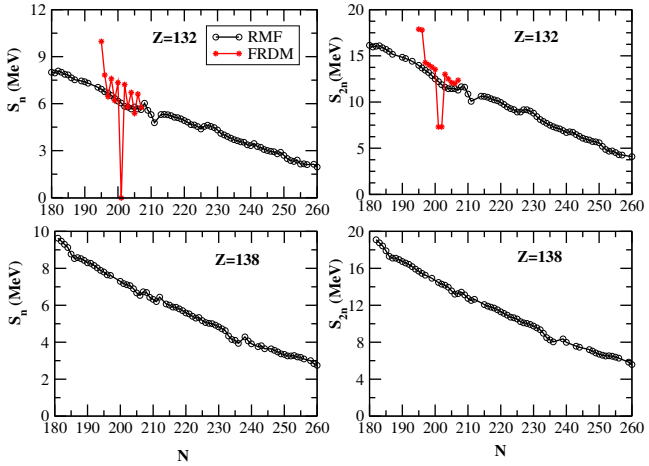

Fig. 4. (Color online) One- and two-neutron separation energies as a function of N.

predicted from the sudden fall in neutron separation energy. Two-neutron separation energy is more interesting because it takes care of even-odd effects. The one- and two-neutron separation energy is calculated by the difference in binding energies of two isotopes using the relations

$$S_n(N,Z) = BE(N,Z) - BE(N-1,Z),$$
$$S_{2n}(N,Z) = BE(N,Z) - BE(N-2,Z). \quad (11)$$

One- and two-neutron separation energy (S_n and S_{2n}) for the considered isotopic series of the nuclei $^{312-392}$132 and $^{318-398}$138 are shown in fig. 4. No sudden fall of the separation energies is observed for both the cases which indicates that as such no neutron magic behaviour within this force parameter is noticed.

Table 2. Same as table 1 but for the $Z = 138$ isotopic chain.

Nuclei	BE			β_2			r_c			r_t		
	sph.	prol.	obl.	sph.	prol.	obl.	sph.	prol	obl.	sph.	prol.	obl.
^{318}138	2081.8	2091.4	2087.4	0.000	0.542	−0.260	6.508	6.809	6.615	6.506	6.788	6.600
^{319}138	2090.9	2101.0	2096.8	0.000	0.546	−0.263	6.513	6.817	6.623	6.513	6.799	6.611
^{320}138	2099.7	2110.5	2106.0	0.000	0.547	−0.266	6.517	6.824	6.631	6.521	6.809	6.621
^{321}138	2108.5	2119.8	2114.9	0.000	0.546	−0.269	6.523	6.829	6.638	6.529	6.816	6.631
^{322}138	2117.1	2128.9	2123.7	0.001	0.544	−0.272	6.528	6.833	6.646	6.538	6.823	6.642
^{323}138	2125.7	2137.7	2132.3	0.001	0.544	−0.275	6.534	6.838	6.653	6.547	6.831	6.652
^{324}138	2134.2	2146.2	2140.7	0.002	0.570	−0.277	6.540	6.868	6.660	6.556	6.863	6.662
^{325}138	2142.6	2154.8	2149.0	0.002	0.592	−0.279	6.547	6.896	6.667	6.565	6.892	6.672
^{326}138	2151.1	2163.3	2157.2	0.003	0.525	−0.280	6.554	6.837	6.673	6.574	6.840	6.681
^{327}138	2159.5	2171.7	2165.3	0.004	0.515	−0.280	6.561	6.834	6.679	6.584	6.840	6.690
^{328}138	2167.9	2180.0	2173.2	0.005	0.508	−0.278	6.568	6.834	6.684	6.593	6.843	6.698
^{329}138	2176.2	2188.3	2181.0	0.003	0.504	−0.272	6.575	6.836	6.686	6.602	6.848	6.702
^{330}138	2184.5	2196.4	2188.9	0.002	0.500	−0.260	6.582	6.839	6.683	6.612	6.854	6.702
^{331}138	2192.9	2204.5	2196.8	0.001	0.497	−0.249	6.589	6.842	6.682	6.621	6.860	6.704
^{332}138	2201.1	2212.4	2204.7	0.001	0.493	−0.245	6.596	6.845	6.685	6.631	6.866	6.709
^{333}138	2209.4	2220.2	2212.4	0.000	0.489	−0.243	6.603	6.848	6.690	6.640	6.871	6.717
^{334}138	2217.6	2227.8	2220.1	0.000	0.484	−0.244	6.610	6.850	6.696	6.649	6.876	6.726
^{335}138	2225.6	2235.4	2227.6	0.000	0.479	−0.244	6.616	6.851	6.703	6.658	6.881	6.735
^{336}138	2233.3	2240.4	2235.0	0.000	0.471	−0.245	6.622	6.851	6.710	6.667	6.883	6.745
^{337}138	2240.7	2250.3	2242.3	0.000	0.465	−0.247	6.628	6.853	6.716	6.676	6.887	6.754
^{338}138	2247.7	2257.6	2249.5	0.000	0.463	−0.248	6.634	6.858	6.723	6.684	6.895	6.764
^{339}138	2254.3	2264.8	2256.7	0.000	0.465	−0.248	6.639	6.867	6.730	6.693	6.907	6.773
^{340}138	2261.1	2272.0	2263.7	0.000	0.470	−0.249	6.645	6.879	6.736	6.701	6.921	6.782
^{341}138	2267.6	2279.0	2270.7	0.001	0.480	−0.250	6.650	6.896	6.743	6.709	6.942	6.791
^{342}138	2274.0	2285.9	2277.0	0.001	0.491	−0.251	6.656	6.914	6.749	6.717	6.962	6.801
^{343}138	2280.5	2292.5	2284.1	0.003	0.506	−0.252	6.661	6.936	6.756	6.726	6.986	6.810
^{344}138	2287.0	2299.1	2290.6	0.010	0.563	−0.254	6.667	6.995	6.762	6.734	7.046	6.820
^{345}138	2293.4	2305.8	2297.0	0.025	0.582	−0.256	6.674	7.020	6.769	6.743	7.072	6.829
^{346}138	2300.0	2312.5	2301.8	0.038	0.589	−0.158	6.681	7.033	6.722	6.753	7.089	6.787
^{347}138	2306.4	2319.0	2308.4	0.050	0.604	−0.157	6.690	7.054	6.728	6.763	7.112	6.795
^{348}138	2312.9	2325.2	2314.8	0.095	0.627	−0.157	6.706	7.078	6.733	6.780	7.139	6.803
^{349}138		2331.4	2321.0		0.650	−0.157		7.103	6.739		7.166	6.812
^{350}138		2337.9	2327.1		0.654	−0.157		7.113	6.744		7.180	6.820
^{351}138		2336.0	2333.2		0.307	−0.158		6.800	6.750		6.879	6.829
^{352}138		2342.1	2339.0		0.255	−0.159		6.771	6.756		6.857	6.838
^{353}138		2348.1	2344.9		0.244	−0.161		6.772	6.762		6.860	6.847
^{354}138		2354.0	2350.7		0.235	−0.162		6.774	6.768		6.865	6.856
^{355}138		2359.9	2356.4		0.230	−0.163		6.778	6.774		6.872	6.864
^{356}138		2365.7	2361.9		0.227	−0.163		6.782	6.779		6.879	6.873
^{357}138		2371.4	2367.4		0.224	−0.163		6.787	6.783		6.887	6.881
^{358}138		2377.0	2372.9		0.221	−0.161		6.791	6.787		6.894	6.888
^{359}138		2382.5	2380.0		0.217	−0.158		6.795	6.757		6.902	6.862
^{360}138		2387.9	2385.8		0.212	−0.151		6.800	6.760		6.909	6.868
^{361}138	2391.5	2393.2		0.019	0.204		6.758	6.803		6.871	6.915	
^{362}138	2397.2	2398.6		0.005	0.183		6.761	6.804		6.877	6.918	
^{363}138	2403.0	2403.7		0.003	0.178		6.765	6.809		6.885	6.924	
^{364}138	2408.8	2408.8		0.002	0.173		6.770	6.813		6.892	6.932	
^{365}138	2414.4	2413.8		0.001	0.166		6.774	6.816		6.900	6.938	
^{366}138	2419.7	2418.8		0.001	0.160		6.779	6.820		6.908	6.945	
^{367}138	2424.8	2423.8		0.001	0.157		6.784	6.825		6.917	6.953	
^{368}138	2429.6	2428.6		0.002	0.156		6.790	6.830		6.926	6.961	
^{369}138	2434.2	2433.3		0.003	0.157		6.795	6.835		6.935	6.970	
^{370}138	2438.8	2437.9		0.005	0.158		6.801	6.839		6.944	6.978	
^{371}138	2443.5	2442.3		0.008	0.158		6.807	6.844		6.954	6.987	
^{372}138	2448.0	2446.4		0.009	0.157		6.813	6.848		6.963	6.995	
^{373}138	2452.6	2450.5		0.006	0.155		6.818	6.852		6.972	7.003	

Table 2. Continued.

Nuclei	BE			β_2			r_c			r_t		
	sph.	prol.	obl.	sph.	prol.	obl.	sph.	prol	obl.	sph.	prol.	obl.
^{374}138	2457.1	2454.5		0.004	0.151		6.824	6.855		6.981	7.010	
^{375}138	2461.6			0.002			6.829			6.989		
^{376}138	2465.9		2465.7	0.002		−0.150	6.833		6.874	6.998		7.032
^{377}138	2469.9		2470.2	0.002		−0.159	6.837		6.883	7.006		7.044
^{378}138	2473.9		2474.7	0.002		−0.167	6.839		6.892	7.014		7.056
^{379}138	2477.7	2473.7	2478.9	0.003	0.192	−0.203	6.841	6.908	6.918	7.021	7.075	7.083
^{380}138	2481.5	2477.5	2483.3	0.004	0.198	−0.214	6.843	6.919	6.930	7.028	7.087	7.097
^{381}138	2485.3	2481.3	2487.7	0.005	0.203	−0.222	6.845	6.929	6.940	7.036	7.100	7.110
^{382}138	2488.9	2484.9	2491.8	0.005	0.207	−0.226	6.847	6.938	6.949	7.043	7.111	7.122
^{383}138	2492.6		2495.5	0.003		−0.229	6.849		6.957	7.051		7.133
^{384}138	2496.3		2499.0	0.003		−0.235	6.852		6.965	7.058		7.145
^{385}138	2499.8		2502.5	0.003		−0.241	6.854		6.975	7.066		7.157
^{386}138	2503.3		2505.9	0.004		−0.246	6.857		6.985	7.075		7.169
^{387}138	2506.7		2509.2	0.004		−0.248	6.860		6.992	7.083		7.180
^{388}138	2509.9		2512.4	0.006		−0.246	6.863		6.996	7.091		7.187
^{389}138	2513.4		2515.5	0.005		−0.239	6.866		6.997	7.100		7.192
^{390}138	2516.6		2518.8	0.004		−0.231	6.868		6.998	7.108		7.196
^{391}138	2519.9		2521.9	0.003		−0.225	6.871		6.999	7.117		7.201
^{392}138	2523.0		2525.3	0.001		−0.222	6.873		7.002	7.125		7.208
^{393}138	2526.3		2528.6	0.001		−0.221	6.876		7.007	7.134		7.216
^{394}138	2529.4		2531.8	0.001		−0.223	6.879		7.014	7.142		7.226
^{395}138	2532.4	2538.7	2534.9	0.000	0.489	−0.226	6.882	7.194	7.021	7.151	7.399	7.236
^{396}138	2535.3	2541.7	2537.8	0.000	0.490	−0.229	6.887	7.201	7.029	7.160	7.409	7.247
^{397}138	2537.9	2544.6	2540.7	0.000	0.490	−0.232	6.893	7.207	7.037	7.170	7.419	7.258
^{398}138	2540.4	2547.3	2543.5	0.000	0.491	−0.235	6.901	7.214	7.045	7.180	7.429	7.269
^{399}138	2542.7	2550.2	2546.2	0.001	0.491	−0.238	6.910	7.222	7.054	7.190	7.439	7.281
^{400}138	2545.1	2553.1	2548.8	0.001	0.492	−0.241	6.919	7.229	7.063	7.200	7.450	7.292
^{401}138	2547.4	2555.9	2551.4	0.003	0.494	−0.245	6.928	7.236	7.072	7.210	7.461	7.303

3.4 Shape coexistence

One of the remarkable properties of nuclear quantum many-body systems is their ability to minimize energy by assuming different shapes at the cost of relatively small energy compared to total binding energy. Generally, the nuclei having different binding energies with different shape configurations correspond to the ground and intrinsic excited states. However, in certain cases it may happen that the binding energy of two different shape configurations may coincide or is very close to each other and this phenomenon is known as shape coexistence [63–65]. This phenomenon is more common in superheavy region giving rise to complex structures in these nuclei and thus enriching our understanding of the oscillations occurring between two or three existing shapes. In the isotopic chains discussed here in the paper, we have come across many examples where the ground and first excited binding energies are degenerate. In the isotopic chain of $^{180-260}$132, we noticed the shape co-existence (oblate-prolate, oblate-spherical) for $^{373-387}$132 and $^{389-396}$132 isotopes as shown in fig. 5. In present analysis, we consider a binding energy difference less or equal to 2 MeV for marking the shape co-existence. Due to this small binding energy difference the ground state can change to low-lying excited state or vice versa by making a small change in the input parameters like the pairing energy. The shape co-existence in nuclei indicates the competition between the different shape configurations differing from each other by a small amount in binding energy so as to acquire the ground state energy with maximum stability and the final shape could be a superposition of these low-lying bands. Further, in the isotopic chain of $^{180-260}$138, we noticed the shape co-existence (oblate-spherical) for $^{379-381}$138 and $^{385-394}$138 as shown in fig. 5. Thus present analysis reveals that some of the nuclei of considered isotopic chain oscillate between oblate-spherical as well as oblate-prolate and vice versa.

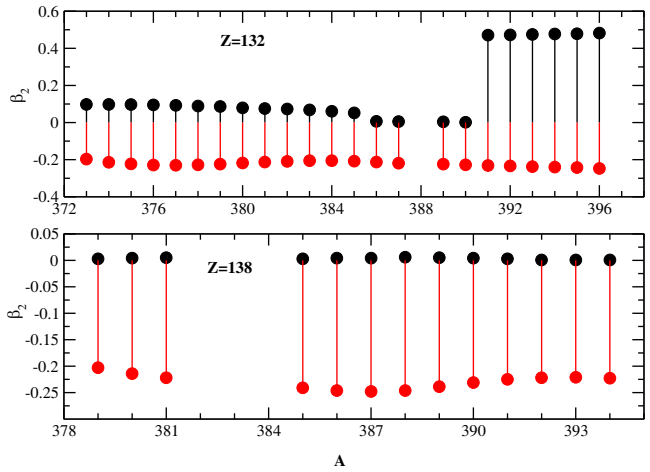

Fig. 5. (Color online) Shape co-existence in $Z = 132$ and $Z = 138$ isotopic chains.

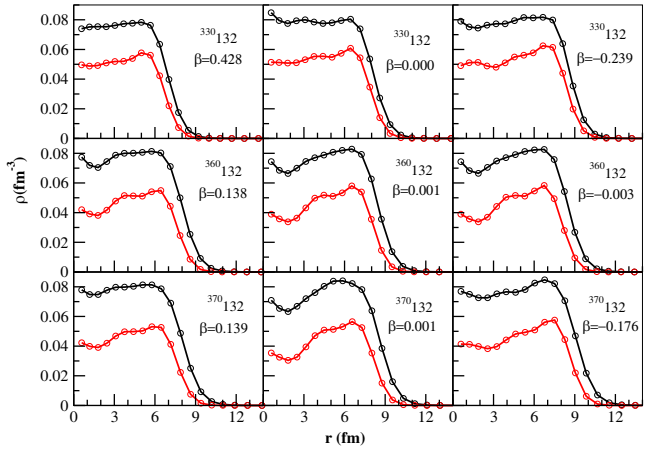

Fig. 6. (Color online) Density profile for some selected nuclei on ground as well as intrinsic excited states. The black line with circle represents the neutron density and proton density is shown by red line with red circle.

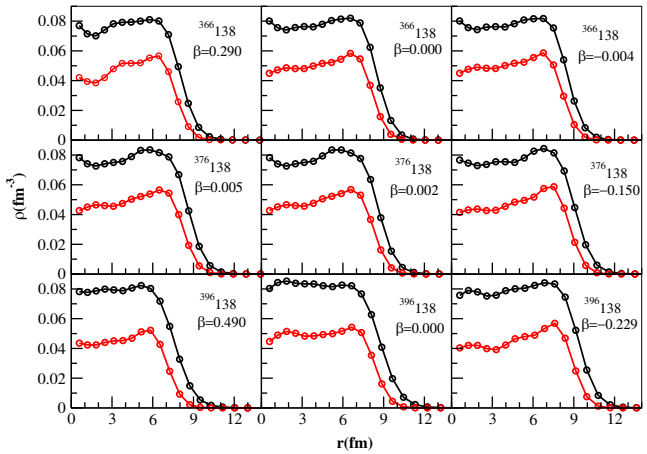

Fig. 7. (Color online) Same as fig. 6 but for $^{366,376,396}138$.

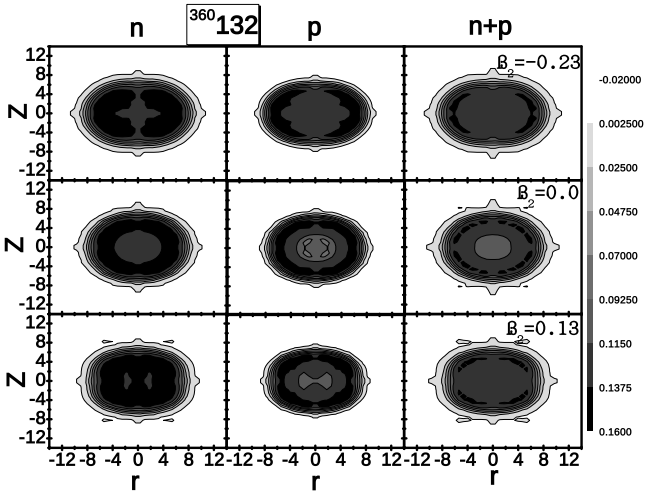

Fig. 8. Two-dimensional neutron, proton and neutron plus proton density contours of $^{360}132$ nucleus for three different shape configurations.

3.5 Density distribution

Density distribution provides a detailed information regarding the distribution of nucleons for identifying central depletion in density, long tails and clusters in density plots. These features are known by bubble, halo and cluster structures of the nuclei and may be observed in light to superheavy nuclei [66–71]. Here, we have plotted the density profile for neutron, proton and total matter (neutron plus proton) for some of the predicted closed shell nuclei [61,62] within this framework as shown in figs. 6, 7. Some of the nuclei, for example, $^{360}132$ and $^{370}132$, show the depletion of central density on ground state as well as intrinsic excited states. The strength of bubble shape is evaluated by calculating the depletion fraction [69,70]. There is no depletion of central density as such for $^{366}138$, $^{376}138$, $^{396}138$ systems. Some nuclei such as $^{360}132$ and $^{370}132$ indicate a special kind of nucleon distribution. In these cases, the centre is slightly bulgy and then afterwards a considerable depletion of nucleon density distribution is noticed which is followed by a big hump between mid of centre and surface of the nuclei. To reveal such type of distribution and to gain an insight into the arrangement of nucleons, we make two-dimensional contour plots for $^{360}132$ and $^{370}132$ with three different shape configurations as given in figs. 8 and 9. Figures 6 and 8 reflect that the hollow region at the centre is spread over the radius of 1–3 fm. This may suggest that these nuclei might have fullerene-type structure and cluster of neutron and alpha-particle might be observed within these types of nuclei. The full black contour refers to maximum density and full white ones to zero density region. It is apparent from fig. 8 that the central portion of total matter density distribution in $^{360}132$ within spherical configuration is less dense than the peripheral region which can be interpreted as a thin gas of nucleons being surrounded by a dense sheath of nucleons (high density) giving rise to a bubble-type structure. The individual neutron and proton density distributions also support the same bubble-like structure within this shape configuration. We witnessed a cluster-type structure in total matter density distribution

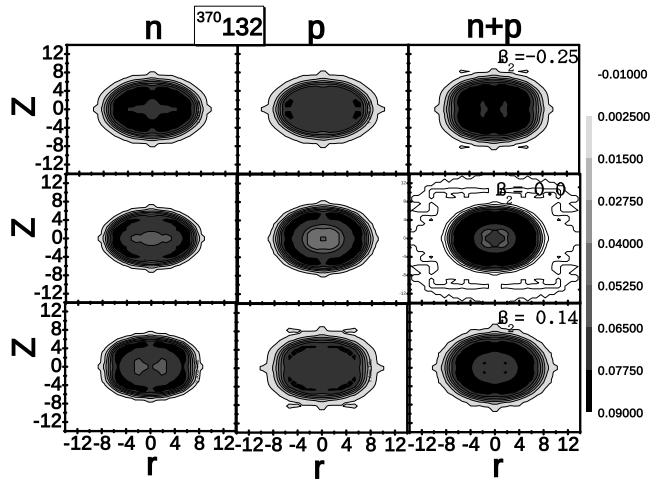

Fig. 9. Same as fig. 8 but for $^{370}132$.

for oblate, spherical and prolate shape configurations. For the case of $^{370}132$ (fig. 9), the two-dimensional contour representation reveals that the total proton density distribution assumes a cluster shape for oblate and prolate configurations with $\beta_2 = -0.25, 0.14$, respectively. In spherical and prolate cases, the proton and total matter density distribution appears to be bubble type, respectively. We noticed a semi-bubble–like structure for the total nucleonic density distribution within the spherical case. The neutron density distribution plot for the oblate shape configuration appears to be spindle shaped with prominent flaps/bulges. Further, inspection reveals that the central part ($r = 0\,\text{fm}$) is considerably populated in proton density distribution while depletion is noticed between $r = 1$ and $r = 3\,\text{fm}$ and further a large population in proton density distribution beyond 3 fm is evident that goes to zero at the surface.

3.6 Decay energy and half-life

In order to predict the modes of decay of the considered nuclides, the α-decay, β-decay and SF half-lives shall be computed using various empirical formulas and their comparison of lifetimes shall predict the dominant mode of decay. To analyze the dominant mode of decay (alpha), the alpha decay half-lives are estimated using various empirical formulas such as Viola-Seaborg (VSS) [72], generalized liquid drop model (GLDM) [73], Brown [74], Royer [75], NI *et al.* [76]. Spontaneous fission half-lives are computed using the semi-empirical formula of Ren and Xu [77] and a comparison with alpha decay half-lives is made in order to predict a possible decay mode of considered nuclides. The beta decay half-lives are estimated using empirical formulas of Fiset and Nix [78].

3.6.1 Alpha decay

A significant advancement has been made for estimating the alpha decay half-lives since the earliest formulation of Geiger and Nuttal [79, 80]. The calculation of α-decay half-life $T^{\alpha}_{\frac{1}{2}}$ requires Q_α as input. The knowledge of Q_α of a nucleus gives a valuable information about its stability. The estimation of Q_α is done by knowing the binding energies of the parent and daughter nuclei and binding energy alpha particle. The binding energies are calculated using the versatile and powerful framework of relativistic mean-field theory. The Q_α energy for the prolate configuration is estimated using the relation

$$Q_\alpha(N,Z) = BE(N-2,Z-2) + BE(2,2) - BE(N,Z). \tag{12}$$

Here, $BE(N,Z)$, $BE(N-2,Z-2)$, and $BE(2,2)$ are the binding energies of the parent, daughter and ^{4}He ($BE = 28.296\,\text{MeV}$ [81]) with neutron number N and proton number Z. With the even-even values available at hand, the alpha decay half-life of the isotopic chain under study is estimated by the Viola-Seaborg semi-empirical relation

$$\log_{10} T^{\alpha}_{\frac{1}{2}} = \frac{aZ-b}{\sqrt{Q_\alpha}} - (cZ+d) + h_{\log}. \tag{13}$$

The values of the parameters a, b, c and d are taken from the recent modified parametrizations of Sobiczewski *et al.* [9], which are $a = 1.66175$, $b = 8.5166$, $c = 0.20$, $d = 33.9069$. The $h_{\log}$ is the hindrance factor which takes into account the hindrance associated with odd proton and neutron numbers as given by Viola and Seaborg

$$h_{\log} = \begin{cases} 0 & \text{even-even;} \\ 0.772 & \text{odd-even;} \\ 1.066 & \text{even-odd;} \\ 1.114 & \text{odd-odd.} \end{cases} \tag{14}$$

The Q_α for the prolate shape obtained from RMF calculations are listed in the tables 3, 4. There are also several phenomenological formulas available in the literature for calculating the alpha decay half-lives. The semi-empirical formula proposed by Brown [74] for determining the half-life of superheavy nuclei is given by

$$\log_{10} T^{\alpha}_{\frac{1}{2}} = 9.54(Z-2)^{0.6}/\sqrt{Q_\alpha} - 51.37, \tag{15}$$

where Z is the atomic number of parent nucleus and Q_α is in MeV. Another formula proposed by Dasgupta-Schubert and Reyes [73] based on generalized liquid drop model and obtained by fitting the experimental half-lives for 373 alpha emitters for determining the half-lives of superheavy nuclei is given as

$$\log_{10} T^{\alpha}_{\frac{1}{2}} = a + bA^{1/6}Z^{1/2} + cZ/Q_\alpha^{1/2}. \tag{16}$$

The parameters a, b and c are given by

$$a,b,c = \begin{cases} -25.31, -1.1629, 1.5864 & \text{even-even;} \\ -26.65, -1.0859, 1.5848 & \text{even-odd;} \\ -25.68, -1.1423, 1.5920 & \text{even-odd;} \\ -29.48, -1.113, 1.6971 & \text{odd-odd.} \end{cases} \tag{17}$$

Table 3. Decay energies for prolate shape and half-lives of α, β and spontaneous fission for $Z = 132$ isotopic chains.

Nuclei	Q_α^{RMF}	Q_α^{FRDM}	$\log(T^\alpha_{1/2})$						$\log(T^{SF}_{1/2})$	Q_β^{RMF}	Q_β^{FRDM}	$\log(T^\beta_{1/2})$	$T^\beta_{1/2}$ (s)	Mode of
	MeV	MeV	FRDM	VSS	GLDM	Brown	Royer	Ni *et al.*	Ren-Xu	MeV	MeV	Fiset-Nix	FRDM	decay
$^{312}132$	17.70			−10.49	−10.33	−9.30	−9.70	−10.82	97.40	11.07		−0.08		α
$^{313}132$	17.50			−9.14	−9.15	−9.06	−9.44	−9.83	83.03	10.86		−0.53		α
$^{314}132$	17.14			−9.68	−9.56	−8.62	−8.93	−10.13	103.83	10.82		−0.02		α
$^{315}132$	16.82			−8.13	−8.19	−8.22	−8.47	−8.97	87.03	10.74		−0.50		α
$^{316}132$	16.68			−8.98	−8.91	−8.04	−8.28	−9.53	105.63	10.5		0.06		α
$^{317}132$	16.51			−7.65	−7.74	−7.81	−8.03	−8.56	86.67	10.21		−0.37		α
$^{318}132$	16.48			−8.67	−8.63	−7.78	−8.00	−9.27	102.89	9.89		0.21		α
$^{319}132$	16.39			−7.46	−7.59	−7.66	−7.88	−8.40	82.01	9.56		−0.20		α
$^{320}132$	16.34			−8.45	−8.45	−7.59	−7.82	−9.08	95.68	8.58		0.57		α
$^{321}132$	16.30			−7.32	−7.48	−7.54	−7.77	−8.28	73.13	8.42		0.12		α
$^{322}132$	16.05			−7.98	−8.02	−7.19	−7.39	−8.68	84.09	8.17		0.69		α
$^{323}132$	15.92			−6.70	−6.90	−7.01	−7.19	−7.75	60.13	8.08		0.22		α
$^{324}132$	14.38			−5.01	−5.10	−4.70	−4.48	−6.14	68.20	7.95		0.76		α
$^{325}132$	14.28			−3.75	−4.00	−4.54	−4.30	−5.23	43.07	7.63		0.36		α
$^{326}132$	14.19	16.01	−7.92	−4.64	−4.77	−4.39	−4.14	−5.82	48.10	7.36	8.70	0.95	0.29	α
$^{327}132$	13.99	12.04	1.22	−3.17	−3.47	−4.05	−3.76	−4.74	22.03	7.07	6.28	0.55	0.81	α
$^{328}132$	13.95	11.57	1.38	−4.16	−4.33	−3.99	−3.70	−5.41	23.85	6.76	4.88	1.16	1.48	α
$^{329}132$	13.84	14.05	−3.30	−2.87	−3.20	−3.80	−3.50	−4.48	−2.92	6.43	5.73	0.78	1.81	α
$^{330}132$	13.75	13.99	−4.23	−3.75	−3.96	−3.64	−3.33	−5.06	−4.46	6.07	4.30	1.42	2.34	SF
$^{331}132$	13.69	13.99	−3.02	−2.56	−2.92	−3.54	−3.22	−4.21	−31.71	5.70	5.16	1.08	1.81	SF
$^{332}132$	13.61	13.85	−3.96	−3.46	−3.71	−3.40	−3.07	−4.82	−36.76	5.34	3.61	1.73	4.28	SF
$^{333}132$	13.53	19.75	−12.10	−2.22	−2.62	−3.26	−2.92	−3.92	−64.27	4.98	10.32	1.40	0.41	SF
$^{334}132$	13.49	19.54	12.92	−3.20	−3.49	−3.19	−2.86	−4.60	−72.99	4.65	3.45	2.06	8.71	SF
$^{335}132$	13.38	13.88	−2.94	−1.90	−2.34	−2.99	−2.64	−3.65	−100.53	4.35	4.12	1.72	15.82	SF
$^{336}132$	13.36	19.20	−12.50	−2.93	−3.25	−2.95	−2.61	−4.36	−113.06	4.14	2.83	2.34	15.69	SF
$^{337}132$	13.14	14.40	−3.45	−1.38	−1.85	−2.55	−2.15	−3.20	−140.42	4.01	4.19	1.91	11.55	SF
$^{338}132$	12.90	14.04	−4.34	−1.91	−2.27	−2.10	−1.64	−3.49	−156.92	3.91	2.70	2.47	18.05	SF
$^{339}132$	12.72	13.33	−1.80	−0.43	−0.94	−1.75	−1.24	−2.39	−183.89	3.71	3.07	2.10	> 100	SF
$^{340}132$	11.98			0.31	−0.11	−0.24	0.52	−1.60	−204.50	3.66		2.63		SF
$^{341}132$	11.76			1.94	1.38	0.24	1.07	−0.37	−230.87	3.16		2.46		SF
$^{342}132$	11.78			0.82	0.37	0.19	1.00	−1.16	−255.72	2.77		3.25		SF
$^{343}132$	12.13			0.99	0.41	−0.56	0.10	−1.18	−281.29	1.99		3.47		SF
$^{344}132$	12.86			−1.82	−2.28	−2.02	−1.64	−3.41	−310.54	2.75		3.27		SF
$^{345}132$	12.29			0.60	−0.02	−0.89	−0.32	−1.52	−335.10	3.12		2.50		SF
$^{346}132$	12.26			−0.39	−0.90	−0.83	−0.27	−2.20	−368.87	2.90		3.16		SF
$^{347}132$	12.06			1.17	0.52	−0.41	0.21	−1.03	−392.24	2.73		2.80		SF
$^{348}132$	11.85			0.64	0.09	0.04	0.72	−1.32	−430.67	2.55		3.44		SF
$^{349}132$	11.64			2.25	1.56	0.50	1.25	−0.10	−452.65	2.35		3.12		SF
$^{350}132$	11.55			1.43	0.84	0.70	1.47	−0.64	−495.88	2.17		3.79		SF
$^{351}132$	11.49			2.66	1.93	0.84	1.62	0.24	−516.28	2.01		3.46		SF
$^{352}132$	11.50			1.56	0.94	0.82	1.58	−0.53	−564.43	1.82		4.16		SF
$^{353}132$	11.52			2.58	1.82	0.77	0.21	0.17	-583.06	1.62		3.90		SF
$^{354}132$	11.66			1.14	0.48	0.46	1.12	−0.89	−636.28	1.42		4.65		SF
$^{355}132$	11.70			2.10	1.31	0.37	1.00	−0.24	−652.96	1.25		4.40		SF
$^{356}132$	11.71			1.00	0.31	0.35	0.96	−1.01	−711.35	−1.05		5.21		SF
$^{357}132$	11.81			1.81	0.99	0.13	0.68	−0.48	−725.91	0.83		5.11		SF
$^{358}132$	11.58			1.35	0.62	0.64	1.27	−0.71	−789.61	0.89		5.50		SF
$^{359}132$	11.21			3.43	2.57	1.49	2.26	0.90	−801.86	0.73		5.32		SF
$^{360}132$	10.83			3.46	2.69	2.41	3.33	1.09	−870.99	0.57		6.18		SF
$^{361}132$	10.45			5.68	4.77	3.38	4.46	2.82	−880.77	0.38		6.20		SF
$^{362}132$	10.11			5.70	4.88	4.29	5.52	3.00	−955.45	0.14		7.61		SF
$^{363}132$	10.07			6.90	5.95	4.40	5.63	3.86	−962.58	−0.15		7.07		SF
$^{364}132$	10.07			5.83	4.98	4.40	5.62	3.11	−1042.94	−0.37		6.73		SF
$^{365}132$	10.08			6.86	5.89	4.37	5.57	3.83	−1047.26	−0.58		5.66		SF
$^{366}132$	10.11			5.70	4.81	4.29	5.46	3.00	−1133.40	−0.75		5.78		SF
$^{367}132$	10.11			6.77	5.76	4.29	5.44	3.75	−1134.74	−0.89		5.01		SF

Table 3. Continued.

Nuclei	Q_α^{RMF}	$\log(T_{1/2}^\alpha)$					$\log(T_{1/2}^{SF})$	Q_β^{RMF}	$\log(T_{1/2}^\beta)$	Mode
	MeV	VSS	GLDM	Brown	Royer	Ni *et al.*	Ren-Xu	MeV	Fiset-Nix	of decay
$^{368}132$	10.12	5.67	4.75	4.26	5.39	2.97	−1226.78	−1.01	5.30	SF
$^{369}132$	10.13	6.70	5.66	4.23	5.34	3.69	−1224.99	−1.15	4.57	SF
$^{370}132$	10.09	5.77	4.82	4.34	5.46	3.06	−1323.05	−1.32	4.82	SF
$^{371}132$	10.10	6.80	5.73	4.32	5.41	3.78	−1317.95	−1.51	4.06	SF
$^{372}132$	10.02	6.00	5.01	4.54	5.66	3.26	−1422.15	−1.66	4.38	SF
$^{373}132$	9.60	8.50	7.39	5.75	7.07	5.23	−1413.60	−2.05	3.45	SF
$^{374}132$	9.29	8.56	7.53	6.69	8.17	5.45	−1524.03	−2.19	3.81	SF
$^{375}132$	8.96	10.89	9.73	7.75	9.41	7.27	−1511.88	−2.34	3.17	SF
$^{376}132$	8.75	10.67	9.59	8.46	10.23	7.24	−1628.66	−2.50	3.53	SF
$^{377}132$	8.80	11.53	10.34	8.29	10.01	7.82	−1612.75	−2.67	2.89	SF
$^{378}132$	8.67	11.00	9.88	8.73	10.52	7.52	−1735.99	−2.83	3.26	SF
$^{379}132$	8.54	12.60	11.37	9.19	11.04	8.73	−1716.17	−2.98	2.65	SF
$^{380}132$	8.43	12.01	10.85	9.58	11.49	8.39	−1845.97	−3.16	3.02	SF
$^{381}132$	8.32	13.55	12.28	9.99	11.95	9.54	−1822.11	−3.33	2.40	SF
$^{382}132$	8.33	12.44	11.26	9.95	11.90	8.76	−1958.57	−3.57	2.75	SF
$^{383}132$	8.43	13.07	11.78	9.58	11.45	9.13	−1930.51	−3.90	2.05	SF
$^{384}132$	8.50	11.71	10.49	9.33	11.14	8.13	−2073.74	−4.16	2.40	SF
$^{385}132$	8.61	12.31	10.99	8.94	10.66	8.48	−2041.35	−4.41	1.76	SF
$^{386}132$	8.49	11.75	10.51	9.37	11.15	8.17	−2191.45	−4.48	2.23	SF
$^{387}132$	8.78	11.61	10.27	8.36	9.94	7.88	−2154.58	−4.83	1.55	SF
$^{388}132$	8.69	10.91	9.64	8.67	10.29	7.45	−2311.65	−5.05	1.95	SF
$^{389}132$	8.62	12.27	10.89	8.91	10.56	8.45	−2270.17	−5.21	1.38	SF
$^{390}132$	3.00	61.12	59.48	50.81	60.04	50.30	−2434.31	−5.15	1.91	SF
$^{391}132$	2.81	66.23	64.41	54.21	64.04	54.51	−2388.08	−5.83	1.11	SF
$^{392}132$	2.73	66.99	65.28	55.74	65.84	55.32	−2559.39	−6.07	1.52	SF

In ref. [76] Ni *et al.* proposed a unified formula for determining the half-lives in alpha decay and cluster radioactivity. The formula for alpha decay is written as

$$\log_{10} T_{1/2}^{\alpha} = 2a\sqrt{\mu}(Z-2)Q_{\alpha}^{-1/2} + b\sqrt{\mu}[2(Z-2)]^{-1/2} + c, \tag{18}$$

where a, b, c are the constants and μ is expressed as $4(A-4)/A$. Recently, Royer estimated the potential energy during α emission within liquid drop model including the proximity effects between α particle and the daughter nucleus and the α-decay half-lives were calculated from the WKB barrier penetration probability analogous to asymmetric spontaneous fission. The theoretical predictions for half-life of heavy and superheavy nuclei by employing a fitting procedure to a set of 373 alpha emitters were developed by Royer [75] with an RMS derivation of 0.42, given as

$$\log_{10} T_{1/2}^{\alpha} = -26.06 - 1.114A^{1/6}\sqrt{Z} + \frac{1.5837Z}{\sqrt{Q_\alpha}}, \tag{19}$$

where A and Z represent, respectively, the mass number and charge number of the parent nuclei and Q_α represents the energy released during the reaction. Assuming a similar dependence on A, Z and Q_α, the above equation was reformulated for a subset of 131 even-even nuclei and a relation was obtained with a RMS derivation of only 0.285, given as

$$\log_{10} T_{1/2}^{\alpha} = -25.31 - 1.1629A^{1/6}\sqrt{Z} + \frac{1.5864Z}{\sqrt{Q_\alpha}}. \tag{20}$$

For a subset of 106 even-odd nuclei, the above equation was further modified with an RMS derivation of 0.39, and is given as

$$\log_{10} T_{1/2}^{\alpha} = -26.65 - 1.0859A^{1/6}\sqrt{Z} + \frac{1.5848Z}{\sqrt{Q_\alpha}}. \tag{21}$$

A similar reformulation was performed for the equation for a subset of 86 odd-even nuclei and 50 odd-odd nuclei.

3.6.2 Beta decay

Beta decay is also a very important decay mode for proton-rich and neutron-rich nuclei. Fermi theory of β decay involves electron-neutrino interaction, which describes

Table 4. Same as table 3 but for the $Z = 138$ isotopic chain.

Nuclei	Q_α^{RMF}	$\log(T_{1/2}^\alpha)$					$\log(T_{1/2}^{SF})$	Q_β^{RMF}	$\log(T_{1/2}^\beta)$	Mode
	MeV	VSS	GLDM	Brown	Royer	Ni *et al.*	Ren-Xu	MeV	Fiset-Nix	of decay
^{318}138	7.62	18.17	18.31	14.50	18.92	13.77	109.15	14.13	−0.68	β
^{319}138	7.10	22.11	22.08	16.87	21.75	16.97	98.02	13.83	−1.12	β
^{320}138	6.52	24.65	24.70	19.84	25.31	19.30	131.77	13.50	−0.56	β
^{321}138	6.05	29.01	28.89	22.56	28.55	22.86	117.23	13.15	−0.99	β
^{322}138	5.58	31.65	31.60	25.61	32.20	25.27	149.00	12.77	−0.42	β
^{323}138	16.86	−6.98	−6.80	−7.09	−7.11	−7.83	131.31	12.37	−0.84	α
^{324}138	17.10	−8.43	−8.17	−7.40	−7.51	−8.90	160.94	11.90	−0.24	α
^{325}138	17.06	−7.30	−7.15	−7.35	−7.46	−8.10	140.38	11.82	−0.72	α
^{326}138	16.93	−8.16	−7.94	−7.18	−7.28	−8.68	167.70	11.57	−0.17	α
^{327}138	16.64	−6.63	−6.52	−6.79	−6.83	−7.53	144.51	11.35	−0.62	α
^{328}138	16.50	−7.46	−7.29	−6.61	−6.62	−8.08	169.36	11.17	−0.08	α
^{329}138	16.29	−6.05	−5.98	−6.32	−6.29	−7.04	143.81	11.02	−0.54	α
^{330}138	16.12	−6.83	−6.69	−6.08	−6.03	−7.54	166.01	10.75	0.02	α
^{331}138	15.99	−5.54	−5.51	−5.90	−5.82	−6.60	138.35	10.47	−0.41	α
^{332}138	15.86	−6.38	−6.29	−5.71	−5.62	−7.16	157.75	10.21	0.15	α
^{333}138	15.76	−5.14	−5.14	−5.57	−5.46	−6.26	128.23	9.97	−0.28	α
^{334}138	15.73	−6.15	−6.10	−5.52	−5.43	−6.96	144.67	9.74	0.27	α
^{335}138	15.63	−4.90	−4.95	−5.38	−5.27	−6.06	113.52	9.51	−0.16	α
^{336}138	18.11	−9.94	−9.89	−8.64	−9.21	−10.19	126.85	9.83	0.25	α
^{337}138	15.61	−4.87	−4.95	−5.35	−5.27	−6.03	94.31	9.06	−0.04	α
^{338}138	15.56	−5.85	−5.87	−5.27	−5.19	−6.70	104.38	8.80	0.53	α
^{339}138	15.52	−4.71	−4.82	−5.21	−5.14	−5.90	70.68	8.50	0.12	α
^{340}138	15.28	−5.33	−5.40	−4.85	−4.72	−6.27	77.33	8.21	0.70	α
^{341}138	15.07	−3.88	−4.03	−4.53	−4.35	−5.19	42.71	7.93	0.29	α
^{342}138	14.82	−4.46	−4.57	−4.14	−3.90	−5.53	45.79	7.63	0.89	α
^{343}138	14.70	−3.17	−3.36	−3.94	−3.68	−4.58	10.46	7.24	0.52	α
^{344}138	14.63	−4.09	−4.24	−3.83	−3.56	−5.21	9.84	6.95	1.12	α
^{345}138	14.27	−2.30	−2.54	−3.24	−2.86	−3.85	−25.97	6.93	0.63	SF
^{346}138	13.90	−2.60	−2.79	−2.60	−2.11	−3.93	−30.44	6.63	1.23	SF
^{347}138	13.98	−1.70	−1.97	−2.74	−2.30	−3.33	−66.53	6.21	0.90	SF
^{348}138	14.06	−2.94	−3.16	−2.88	−2.48	−4.22	−75.00	5.88	1.53	SF
^{349}138	13.96	−1.66	−1.96	−2.70	−2.29	−3.30	−111.14	5.60	1.15	SF
^{350}138	13.47	−1.66	−1.93	−1.83	−1.25	−3.13	−123.73	5.59	1.65	SF
^{351}138	21.29	−12.90	−13.13	−11.96	−13.45	−12.88	−159.73	4.78	1.52	SF
^{352}138	21.00	−13.64	−13.84	−11.69	−13.14	−13.35	−176.59	5.96	1.50	SF
^{353}138	14.25	−2.26	−2.63	−3.20	−2.95	−3.81	−212.23	5.42	1.23	SF
^{354}138	14.19	−3.21	−3.53	−3.10	−2.85	−4.45	−233.50	5.23	1.81	SF
^{355}138	14.12	−1.99	−2.39	−2.98	−2.72	−3.58	−268.58	5.03	1.41	SF
^{356}138	14.04	−2.89	−3.25	−2.84	−2.57	−4.19	−294.38	4.82	2.01	SF
^{357}138	13.96	−1.66	−2.09	−2.70	−2.42	−3.30	−328.72	4.61	1.62	SF
^{358}138	13.86	−2.51	−2.91	−2.53	−2.23	−3.86	−359.18	4.39	2.23	SF
^{359}138	13.77	−1.25	−1.72	−2.37	−2.05	−2.95	−392.57	4.17	1.86	SF
^{360}138	13.75	−2.27	−2.71	−2.33	−2.03	−3.66	−427.82	3.92	2.50	SF
^{361}138	13.68	−1.06	−1.56	−2.21	−1.89	−2.78	−460.08	3.66	2.16	SF
^{362}138	13.45	−1.61	−2.09	−1.79	−1.40	−3.10	−500.25	3.55	2.73	SF
^{363}138	13.32	−0.26	−0.80	−1.55	−1.13	−2.10	−531.19	3.28	2.41	SF
^{364}138	18.19	−10.05	−10.48	−8.74	−9.79	−10.29	−576.40	3.03	3.09	SF
^{365}138	13.17	0.09	−0.49	−1.27	−0.82	−1.81	−605.83	2.86	2.72	SF
^{366}138	13.05	−0.70	−1.24	−1.04	−0.56	−2.32	−656.21	2.75	3.31	SF
^{367}138	12.96	0.58	−0.03	−0.86	−0.37	−1.39	−683.96	2.62	2.92	SF
^{368}138	12.97	−0.51	−1.09	−0.88	−0.41	−2.16	−739.63	2.44	3.57	SF
^{369}138	13.03	0.41	−0.23	−1.00	−0.56	−1.53	−765.51	2.24	3.26	SF
^{370}138	13.10	−0.82	−1.43	−1.13	−0.74	−2.42	−826.58	1.98	4.01	SF
^{371}138	13.30	−0.21	−0.88	−1.51	−1.21	−2.06	−850.43	1.64	3.90	SF
^{372}138	13.52	−1.77	−2.41	−1.92	−1.72	−3.23	−917.02	1.33	4.81	SF
^{373}138	13.58	−0.84	−1.53	−2.03	−1.86	−2.60	−938.66	1.14	4.59	SF

Table 4. Continued.

Nuclei	Q_α^{RMF}	$\log(T_{1/2}^\alpha)$					$\log(T_{1/2}^{SF})$	Q_β^{RMF}	$\log(T_{1/2}^\beta)$	Mode
	MeV	VSS	GLDM	Brown	Royer	Ni *et al.*	Ren-Xu	MeV	Fiset-Nix	of decay
^{374}138	13.69	−2.14	−2.81	−2.23	−2.12	−3.55	−1010.89	1.01	5.31	SF
^{375}138	10.54	7.26	6.46	4.64	6.12	4.31	−1030.16	1.59	3.97	SF
^{376}138	10.12	7.59	6.81	5.79	7.48	4.75	−1108.13	1.09	5.18	SF
^{377}138	9.92	9.35	8.50	6.36	8.16	6.09	−1124.86	0.76	5.28	SF
^{378}138	12.47	0.71	−0.05	0.12	0.64	−1.12	−1208.70	0.31	6.94	SF
^{379}138	16.40	−6.23	−6.96	−6.47	−7.30	−7.20	−1222.72	0.10	7.37	SF
^{380}138	16.24	−7.03	−7.75	−6.25	−7.05	−7.71	−1312.53	−0.05	8.28	SF
^{381}138	16.01	−5.57	−6.34	−5.93	−6.67	−6.63	−1323.69	−0.22	6.78	SF
^{382}138	15.94	−6.52	−7.27	−5.83	−6.57	−7.28	−1419.59	−0.44	6.55	SF
^{383}138	11.78	3.58	2.69	1.61	2.35	1.17	−1427.72	−0.48	5.95	SF
^{384}138	11.53	3.21	2.33	2.18	3.02	1.01	−1529.80	−0.33	6.89	SF
^{385}138	11.43	4.56	3.63	2.41	3.29	2.00	−1534.76	−0.49	5.92	SF
^{386}138	11.28	3.92	3.01	2.77	3.70	1.62	−1643.14	−0.65	6.03	SF
^{387}138	11.21	5.19	4.23	2.94	3.89	2.55	−1644.77	−0.78	5.26	SF
^{388}138	11.12	4.39	3.45	3.16	4.14	2.03	−1759.55	−0.90	5.52	SF
^{389}138	11.09	5.55	4.56	3.23	4.21	2.85	−1757.70	−1.00	4.85	SF
^{390}138	11.01	4.72	3.74	3.43	4.43	2.31	−1878.98	−1.10	5.18	SF
^{391}138	10.81	6.40	5.37	3.93	5.02	3.58	−1873.50	−1.18	4.56	SF
^{392}138	10.65	5.84	4.82	4.35	5.51	3.26	−2001.38	−1.26	4.94	SF
^{393}138	10.43	7.61	6.54	4.93	6.19	4.61	−1992.14	−1.35	4.31	SF
^{394}138	10.27	7.08	6.02	5.37	6.70	4.32	−2126.72	−1.46	4.66	SF
^{395}138	3.82	52.22	50.69	41.66	50.31	42.64	−2113.56	−4.78	1.59	SF
^{396}138	3.70	52.97	51.48	43.16	52.10	43.44	−2254.94	−3.08	3.10	SF
^{397}138	3.68	54.35	52.77	43.42	52.39	44.46	−2237.73	−3.31	2.44	SF
^{398}138	9.52	9.74	8.59	7.56	9.28	6.59	−2386.00	−3.47	2.83	SF

the beta transition rates according to $\log(ft)$ values. We employed the empirical formula of Fiset and Nix [78] for estimating the half-lives of the isotopic chain under study and is given as

$$T_{1/2}^{\beta} = 540 \times 10^{5.0} \frac{m_e^5}{\rho_{d.o.s.}(W_\beta^6 - m_e^6)}\,. \tag{22}$$

In an analogous way to α-decay, we evaluate the Q_β value using the relation $Q_\beta = BE(Z+1, A) - BE(Z, A)$ and $W_\beta = Q_\beta + m_e$ Here, $\rho_{d.o.s.}$ is the average density of states in the daughter nucleus ($e^{-A/290}\times$ number of states within 1 MeV of ground state).

3.6.3 Spontaneous fission

The determination of spontaneous half-lives helps in identifying the long-lived superheavy elements and mode of decay of heavy and superheavy nuclei. Several empirical formulas have been proposed by various authors from time to time for determining the spontaneous fission half-lives. In our calculations, we employed the phenomenological formula proposed by Ren and Xu [77] expressed as

$$\begin{aligned}\log_{10} T_{1/2}^{SF} = {} & 21.08 + \mathrm{C}_1 \frac{(Z-90-\nu)}{A} + \mathrm{C}_2 \frac{(Z-90-\nu)^2}{A} \\ & + \mathrm{C}_3 \frac{(Z-90-\nu)^3}{A} \\ & + \mathrm{C}_4 \frac{(Z-90-\nu)(N-Z-52)^2}{A}\,,\end{aligned} \tag{23}$$

where, Z, N, A represent the proton, neutron and mass number of parent nuclei. C_1, C_2, C_3, C_4 are the empirical constants and ν is the seniority term which takes care of blocking effect of unpaired nucleons on the transfer of many nucleon pairs during the fission process.

Our study on modes of decay highlights the range of isotopes which survive fission and thus decay through alpha emission. Alpha and beta decay energies, Q_α, Q_β estimated by RMF binding energy are in quite agreement with FRDM data as given in table 3. However, calculated half-lives by RMF do not match well with FRDM values. The reason for disagreement is that $T_{1/2}^{\alpha} \propto 10^{\frac{1}{\sqrt{Q_\alpha}}}$ and

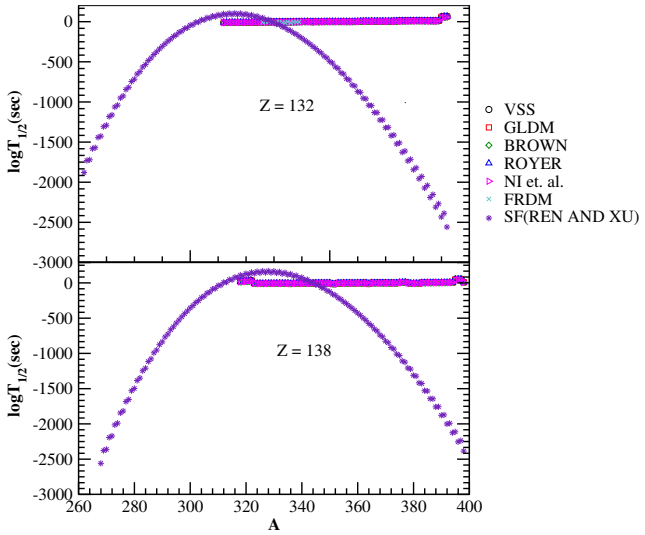

Fig. 10. (Color online) Alpha decay and spontaneous fission half-lives of $Z = 132$, 138 isotopic chains as a function of mass number.

$T^{\beta}_{1/2}$ is nearly proportional to $\frac{1}{Q_{\beta}{}^{6}}$ indicating that a small change in Q_{α} and Q_{β} creates a big difference in $T^{\alpha}_{1/2}$ and $T_{1/2}\beta$ as reflected in tables 3, 4. The calculated alpha decay half-lives using VSS, GLDM, Brown, Royer and NI *et al.* are tabulated in tables 3, 4 and a good agreement among them as well as with macro-microscopic data is noticed. To check the possibility of β-decay empirical Fiset and Nix formula is employed to calculate the β-decay half-life for the considered isotopic chain and the results are given in tables 3, 4. The beta decay half-lives are found to be very large than alpha decay as well as spontaneous fission half-lives and hence there is no possibility of beta decay in the present considered isotopes. Further, SF half-lives are calculated and the values are framed in one of the columns of tables 3, 4. Also, the alpha decay and SF half-lives for considered isotopic chain are plotted in fig. 10. After analyzing the concerned tables and figure, the analysis predicts that the isotopes of $Z = 132$ with a mass range $312 \leq A \leq 329$ survive the fission and may be observed through alpha decay and those nuclei beyond $A > 329$ do not survive the fission and hence completely undergo spontaneous fission. For $Z = 138$, the nuclides with a mass range $323 \leq A \leq 344$ survive the fission and are observed through alpha decay in the laboratory while the nuclei beyond $A > 344$ do not survive fission and end with spontaneous fission. In the first five isotopes $^{318-322}138$, beta decay is the dominant mode of decay. Therefore, the present study reveals that alpha decay and spontaneous fission are the principal modes of decay of majority of the considered nuclides with β decay as the principal mode of decay in first five isotopes of $Z = 138$.

4 Summary

We calculated the structural properties of $Z = 132, 138$ superheavy nuclei with a neutron range of $N = 180$–260 within axially deformed relativistic mean-field theory. The calculations are performed for prolate, oblate and spherical configurations in which prolate configuration is suggested to be ground state. The results produced by RMF are in good agreement with FRDM data. Density distribution has been plotted to explain the special features of the nuclei such as bubble structure or halo structure. Bubble structure is seen for some of the isotopes of nuclei under investigation. To make clear presentation of nucleon distribution for some of the selected nuclei, the two-dimensional contour plot of density has been made by which cluster- and bubble-type structure is revealed. Further, the predictions of possible modes of decay such as alpha decay, beta decay and spontaneous fission of the isotopes of $Z = 132$ and $Z = 138$ in the neutron range $180 \leq N \leq 260$ have been made within self-consistent model. The half-lives computed using Viola-Seaborg, GLDM, Brown, Royer and Ni *et al.*, show good agreement with each other as well as with macro-microscopic FRDM data. All the physical observables calculated by RMF are found in good agreement with FRDM data. Also, an extensive study on beta decay half-lives and SF half-lives of the considered isotopic chain under investigations has been carried out to identify the mode of the decay of these isotopes. The study reveals that the isotopes of $Z = 132$ that fall within the mass range $312 \leq A \leq 329$ undergo alpha decay and those with mass number $A > 329$ do not survive fission and hence completely undergo spontaneous fission. For $Z = 138$, the alpha decay occurs within the isotopic mass chain $318 \leq A \leq 344$ and the isotopes beyond $A > 344$ do not survive fission and end up with spontaneous fission. The present analysis reveals that α-decay and SF are the principal modes of decay in majority of the isotopes of superheavy nuclei under study in addition to β-decay being the principal mode of decay in $^{318-322}138$ isotopes. Hence, we hope that the present theoretical predictions on possible decay modes of $Z = 132$, 138 superheavy nuclei might pave the way to help and guide the experimentalists in near future for the synthesis of new superheavy isotopes.

One of the authors (MI) would like to acknowledge the hospitality provided by the Institute of Physics (IOP), Bhubaneswar during the work. AAU acknowledges the Inter University Centre for Astronomy and Astrophysics for the Associateship.

References

1. W.D. Myers, W.J. Swiatecki, Nucl. Phys. A **81**, 1 (1966).
2. A. Sobiczewski, F.A. Gareev, B.N. Kalinkin, Phys. Lett. **22**, 500 (1966).
3. H. Meldner, Ark. Fys. **36**, 593 (1967).
4. S.G. Nilsson, C.F. Tsang, A. Sobiczewski, Z. Szymanski, S. Wycech, C. Gustafson, I.L. Lamm, P. Möller, B. Nilsson, Nucl. Phys. A **131**, 1 (1969).
5. U. Mosel, W. Greiner, Z. Phys. **222**, 261 (1969).
6. P. Möller, J.R. Nix, W.D. Wyers, W.J. Swiatecki, At. Data Nucl. Data Tables **59**, 185 (1999).
7. P. Möller, J.R. Nix, K.L. Kratz, At. Data Nucl. Data Tables **66**, 131 (1997).

8. S.C. Cwiok, V.V. Pashkevich, J. Dudek, W. Nazarewicz, Nucl. Phys. A **41**, 254 (1983).
9. A. Sobiczewski, Z. Patyk, S.C. Cwiok, Phys. Lett. B **224**, 1 (1989).
10. Z. Patyk, A. Sobiczewski, Nucl. Phys. A **533**, 132 (1991).
11. D.N. Poenaru, M. Ivascu, A. Sandalescu, W. Greiner, Phys. Rev. C **32**, 572 (1985).
12. B. Buck, A.C. Merchant, S.M. Perez, Phys. Rev. C **45**, 2247 (1992).
13. D.N. Basu, Phys. Lett. B **566**, 90 (2003).
14. H.F. Zhang, G. Royer, Phys. Rev. C **76**, 047304 (2007).
15. M.M. Sharma, A.R. Farhan, G. Munzenberg, Phys. Rev. C **71**, 054310 (2005).
16. J.C. Pei, F.R. Xu, Z.J. Lin, E.G. Zhao, Phys. Rev. C **76**, 044326 (2007).
17. S. Hoffman, G. Munzenberg, Rev. Mod. Phys. **72**, 733 (2000).
18. S. Hoffman *et al.*, Z. Phys. A **350**, 277 (1995).
19. S. Hoffman *et al.*, Z. Phys. A **358**, 125 (1997).
20. S. Hoffman *et al.*, Z. Phys. A **350**, 281 (1995).
21. S. Hoffman *et al.*, Z. Phys. A **354**, 229 (1996).
22. S. Hoffman, G. Munzenberg, Rev. Mod. Phys. **72**, 733 (2000).
23. K. Morita *et al.*, J. Phys. Soc. Jpn. **73**, 2593 (2004).
24. K. Morita *et al.*, Nucl. Phys. A **734**, 101 (2004).
25. Yu.Ts. Oganessian *et al.*, Phys. Rev. Lett. **109**, 162501 (2012).
26. Yu.Ts. Oganessian *et al.*, Phys. At. Nucl. **64**, 1349 (2001).
27. Yu.Ts. Oganessian *et al.*, Phys. Rev. C **72**, 034611 (2005).
28. Yu.Ts. Oganessian *et al.*, Phys. At. Nucl. **63**, 1679 (2000).
29. Yu.Ts. Oganessian, J. Phys. G: Nucl. Part. Phys. **34**, R165 (2007).
30. J. Dvorak *et al.*, Phys. Rev. Lett. **97**, 242501 (2006).
31. Yu.Ts. Oganessian *et al.*, Phys. Rev. C **79**, 024603 (2009).
32. D.N. Poenaru *et al.*, At. Data Nucl. Data Tables **34**, 423 (1986).
33. D.N. Poenaru, I.H. Plonski, W. Greiner, Phys. Rev. C **74**, 014312 (2006).
34. D.N. Poenaru, I.H. Plonski, R.A. Ghergesu, W. Greiner, J. Phys. G: Nucl. Part. Phys. **32**, 1223 (2006).
35. C. Samanta, D.N. Basu, P.R. Chowdhary, J. Phys. Soc. Jpn. **76**, 124201 (2007).
36. D.S. Delin, R.J. Liotta, R. Wyss, Phys. Rev. C **76**, 044301 (2007).
37. H.J. Rose, G.A. Jones, Nature **307**, 245 (1984).
38. E. Hourani, M. Hussonnois, D.N. Poenaru, Ann. Phys. (Paris) **14**, 311 (1989).
39. A. Sandulescu, D.N. Poenaru, W. Greiner, Sov. J. Nucl. Phys. **11**, 528 (1980).
40. B.K. Sharma, P. Arumugam, S. K. Patra, P.D. Stevenson, R.K. Gupta, W. Greiner, J. Phys. G **32**, L1 (2006).
41. C. Qi, F.R. Xu, R.J. Liotta, R. Wyss, Phys. Rev. Lett. **103**, 072501 (2009).
42. D.N. Poenaru, R.A. Gherghescu, W. Greiner, Phys. Rev. C **83**, 014601 (2011).
43. D.N. Poenaru, R.A. Gherghescu, W. Greiner, Phys. Rev. Lett. **107**, 062503 (2011).
44. D.N. Poenaru, R.A. Gherghescu, W. Greiner, J. Phys. G **39**, 015105 (2012).
45. D.N. Poenaru, R.A. Gherghescu, W. Greiner, Phys. Rev. C **85**, 034615 (2012).
46. A.V. Karpov, V.I. Zagrebaev, Int. J. Mod. Phys. E **21**, 1250013 (2012).
47. N. Bohr, J.A. Wheeler, Phys. Rev. **56**, 426 (1939).
48. G.N. Flerov, K.A. Petrjak, Phys. Rev. **58**, 89 (1940).
49. W.J. Swiatecki, Phys. Rev. **100**, 937 (1955).
50. Z. Ren, C. Xu, Nucl. Phys. A **759**, 64 (2005).
51. C. Xu, Z. Ren, Phys. Rev. C **71**, 014309 (2005).
52. C. Xu, Z. Ren, Y. Guo, Phys. Rev. C **78**, 044329 (2008).
53. B.D. Serot, Rep. Prog. Phys. **55**, 1855 (1992).
54. Y.K. Gambhir, P. Ring, A. Thimet, Ann. Phys. (N.Y.) **198**, 132 (1990).
55. P. Ring, Prog. Part. Nucl. Phys. **37**, 193 (1996).
56. B.D. Serot, J.D. Walecka, Adv. Nucl. **16**, 1 (1986).
57. J. Boguta, A.R. Bodmer, Nucl. Phys. A **292**, 413 (1977).
58. T. Sil, S.K. Patra, B.K. Sharma, M. Centelles, X. Viñas, Phys. Rev. C **69**, 044315 (2004).
59. D.G. Madland, R.J. Nix, Nucl. Phys. A **476**, 1 (1988).
60. G.A. Lalazissis, S. Karatzikos, R. Fossion, D. Pena Arteaga, A.V. Afanasjev, P. Ring, Phys. Lett. **671**, 36 (2009).
61. W. Zhang, J. Meng, S.Q. Zhang, L.S. Gang, H. Toki, Nucl. Phys. A **753**, 106 (2005).
62. M. Bhuyan, S.K. Patra, Mod. Phys. Lett. A **27**, 1250173 (2012).
63. S.K. Patra, C.R. Praharaj, Phys. Rev. C **47**, 2978 (1993).
64. F. Sarazin *et al.*, Phys. Rev. Lett. **84**, 5062 (2000).
65. J.L. Egido, L.M. Robeldo, R.R. Rodriguez-Guzman, Phys. Rev. lett. **93**, 282502 (2004).
66. J.A. Wheeler, unpublished.
67. H.A. Wilson, Phys. Rev. C **69**, 538 (1946).
68. J. Decharge *et al.*, Nucl. Phys. A **716**, 55 (2003).
69. M. Grasso *et al.*, Phys. Rev. C **79**, 034318 (2009).
70. S.K. Singh, M. Ikram, S.K. Patra, Int. J. Mod. Phys. E **22**, 1350001 (2013).
71. B.K. Sharma, P. Arumugam, S.K. Patra, P.D. Stevenson, R.K. Gupta, W. Greiner, J. Phys. G: Nucl. Part. Phys. **32**, L1 (2006).
72. V.E. Viola jr., G.T. Seaborg, J. Inorg. Nucl. Chem. **28**, 741 (1966).
73. N. Dasgupta-Schubert, M.A. Reyes, At. Data Nucl. Data Tables **93**, 90 (2007).
74. B.A. Brown, Phys. Rev. C **46**, 811 (1992).
75. G. Royer, J. Phys. G: Nucl. Part. Phys. **26**, 1149 (2000).
76. D.D. Ni, Z.Z. Dong, T.K. *et al.*, Phys. Rev. C **78**, 044310 (2008).
77. Z. Ren, C. Xu, Nucl. Phys. A **759**, 64 (2005).
78. E.O. Fiset, J.R. Nix, Nucl. Phys. A **193**, 647 (1972).
79. H. Geiger, J.M. Nuttall, Philos. Mag. **22**, 613 (1911).
80. H. Geiger, Z. Phys. **8**, 45 (1922).
81. G. Audi, A.H. Wapstra, C. Thibault, Nucl. Phys. A **729**, 337 (2003).